

Spatial and Seasonal Variations of Surface PM10 Concentration and MODIS Aerosol Optical Depth over China

Chang-Keun Song¹, Chang-Hoi Ho², Rokjin J. Park², Yong-Sang Choi²,
Jhoon Kim³, Dao-Yi Gong⁴, and Yun-Bok Lee⁵

¹Global Environment Research Center, National Institute of Environmental Research, Incheon, Korea

²School of Earth and Environmental Sciences, Seoul National University, Seoul, Korea

³Department of Atmospheric Sciences, Yonsei University, Seoul, Korea

⁴State Key Laboratory of Earth Surface Processes and Resource Ecology, College of Resources Science and Technology, Beijing Normal University, Beijing, China

⁵Meteorological Observation Standardization Division, Korea Meteorological Administration, Seoul, Korea

(Manuscript received 4 September 2008; in final form 5 January 2009)

Abstract

We examine the spatial and temporal variabilities of ground-observed concentrations of particulate matter with diameters $\leq 10 \mu\text{m}$ (PM10) over China and compare them with satellite-retrieved data on the aerosol optical depth (AOD) collected over the period 2003–2005 using a moderate resolution imaging spectroradiometer (MODIS). Annual mean values of the PM10 concentrations and AOD show a strong spatial correlation, indicating the consistent presence of aerosol concentrations. However, the temporal correlation between the monthly values of the PM10 concentrations and AOD indicates a regional contrast in their seasonality. The correlation coefficients are 0.6 or higher in the southeastern coast region, whereas they are -0.6 or lower in the north-central region. The regional discrepancy is most likely due to the difference in the size distributions of aerosols. This is also supported by the data on the distribution of the Angstrom exponent and fine mode fraction obtained from the MODIS. The characteristics of the aerosols with respect to coarse and fine particles are discussed in this study.

Key words: PM10, aerosol, mass concentration, optical depth, MODIS, China

1. Introduction

There are numerous proposals to use aerosol optical observations retrieved by satellites to estimate the surface particulate matter (PM) concentrations because of the cost effectiveness and spatial coverage of satellites (Engel-Cox *et al.*, 2004, 2005; Liu *et al.*, 2004; Al-Saadi *et al.*, 2005; van Donkelaar *et al.*, 2006). Many previous studies have focused on the United States and Europe, where the ground PM observations are relatively abundant, to validate the satellite-retrieved aerosol concentrations (e.g., Chu *et al.*, 2003; Wang and Christopher, 2003; Al-Saadi *et*

al., 2005). Over East Asia, the air quality is worsening due to the recent booming economic growth in China (Richter *et al.*, 2005; Chan and Yao, 2008); the rapid increase in industrial and agricultural activities during recent decades has led to a significant addition of anthropogenic fine aerosols. In addition, the coarse particles that originated from the arid regions in China have a significant impact on the aerosol budgets in East Asia (Bergin *et al.*, 2001; Wang *et al.*, 2001; Menon *et al.*, 2002). However, the sparse observations of surface PM concentrations left the satellite data as only means without their extensive validation. These motivate the present study.

The authors demonstrate new data sets of PM observations based on the Chinese air pollution index (API) data together with the aerosol optical depth (AOD) obtained from the moderate resolution imaging spectrometer (MODIS) and examine the spatial and temporal relationships between the two in-

Corresponding Author: Chang-Hoi Ho, Climate Physics Laboratory, School of Earth and Environmental Sciences, Seoul National University, Seoul 151-742, Korea.
Phone : +82-2-880-8861, Fax : +82-2-876-6795
E-mail: hoch@cpl.snu.ac.kr

dependent data sets. In 1997, the API in China was first used to measure the effects of pollutant concentrations on human health (Gong *et al.*, 2007). Initially, the pollutants included the concentrations of the total suspended particulates (TSP), sulfur dioxide (SO₂), and nitrogen oxides (NO_x). Later, since 2002, TSP has been replaced with PM₁₀ (diameter ($d \leq 10 \mu\text{m}$) concentrations. Currently, a total of 47 sites routinely measure daily values of the API.

The MODIS installed on board the Terra and Aqua satellites has achieved great success in the systematic retrieval of aerosol products over land (Kaufman *et al.*, 1997; Remer *et al.*, 2005), particularly with regard to the local PM_{2.5} concentrations ($d \leq 2.5 \mu\text{m}$) (Chu *et al.*, 2003; Wang and Christopher, 2003; Al-Saadi *et al.*, 2005). The retrieval of coarse dust particles over desert areas, however, shows the limitation of having to use surface reflectance values measured at $2.1 \mu\text{m}$ because the bright surface areas against dark pixels may result in the underestimation of AOD (Kaufman *et al.*, 1997, 2002a, 2002b).

In order to address the locality of surface aerosol distribution and the potential to establish a link between the PM₁₀ mass concentration and the MODIS-derived AOD values obtained over China, we present a comparison between the MODIS column AOD and the surface PM₁₀ mass concentration observed from the API data at 47 sites (Section 3). The detailed information of data and research regions can be found in the next section. We also explain how a significant discrepancy between the two different aerosol observations takes place on seasonal variations (Section 4). Section 5 finally gives concluding remarks.

2. Description of data and region

The daily averaged API data obtained over three years (2003–2005), are collected from 47 ground-base air quality monitoring sites in main land China (Fig. 1). At each observation site, the concentrations of PM₁₀, SO₂, and NO₂ are automatically obtained. It is noted that the day on which the API is < 50 (i.e., $\text{PM}_{10} < 50 \mu\text{g m}^{-3}$, $\text{SO}_2 < 50 \mu\text{g m}^{-3}$, and $\text{NO}_2 < 80 \mu\text{g m}^{-3}$) is defined as “clean”, and no pollutant type

was recorded on this day. In particular, for PM₁₀, the β -ray absorption or the tapered element oscillation microbalance method is used to measure its mass concentration and the daily average is calculated when values for more than 12 hours in a single day are available. Then, they are converted into the final value of the API for being released to the public; this value is available online at <http://english.sepa.gov.cn>. In this study, the API originating particularly from PM₁₀ was selected and converted into the mass concentration of PM₁₀ by using the inversed equation provided by the Chinese national environmental protection agency. The proportion of PM₁₀-polluted days and clean days to the total days is 93%, 96%, 94%, and 84% in spring, summer, fall, and winter, respectively. The average and variation of PM₁₀ concentration converted from the API in the Chinese cities shows reasonable spatial and temporal distributions (Zhou *et al.*, 2007; Choi *et al.*, 2008a), and significant relationship with meteorological fields such as temperature and precipitation (Gong *et al.*, 2007; Choi *et al.*, 2008b). Details on the API data and conversion method into PM₁₀ concentration can be found elsewhere (Gong *et al.*, 2007; Choi *et al.*, 2008a, 2008b).

The optical observations such as AOD at $0.55 \mu\text{m}$ (AOD_{0.55}), Ångström exponent (\AA), and the fine mode fraction (η) at $0.55 \mu\text{m}$ ($\eta_{0.55}$) are employed in MODIS/Terra Level-3 daily gridded atmospheric data product (MOD08). MOD08 is stored in a $1^\circ \times 1^\circ$ latitude and longitude resolution. Two values — AOD_{0.66} and AOD_{0.47} — are derived independently over land and these are interpolated into the value at $0.55 \mu\text{m}$ using the Ångström law. The value of AOD_{0.55} is reported to have an accuracy level of ± 0.05 plus (or minus) the product of 0.15 and AOD_{0.55} over land (Remer *et al.*, 2005). The \AA value, which has an inverse relation with the particle size, is defined over land for wavelengths of 0.47 and $0.66 \mu\text{m}$ (i.e., $-\ln(\text{AOD}_{0.66}/\text{AOD}_{0.47})/\ln(0.66/0.47)$). The \AA value is averaged by using quality assessment weights in MOD08. The $\eta_{0.55}$ value indicates the ratio of the AOD obtained from the fine mode contribution to the total optical depth (i.e., $\text{AOD}_{0.55}^f/\text{AOD}_{0.55}^{\text{tot}}$, where “f” and “tot” represent the fine mode and the total

AOD, respectively). In practice, MODIS FMF is usually either 0 or 1 over land (Remer *et al.*, 2005). This implies that η over land can be only a qualitative measure.

To investigate the difference and locality in the spatial and temporal patterns of the observed API and MODIS AOD values, we further divide the analysis domain comprising 47 API measurement sites into 8 regions by considering their geographical locations, the different aerosol source regions, and the prevailing climate (Fig. 1). Northwest China (NWC) and North China (NC) are categorized as the most arid areas with an annual rainfall of less than 600 mm and are known as one of the largest dust aerosol source regions in the world. Xuan and Sokolik (2001) estimated the amount of the dust emission from northern China and identified that 36% of the total mineral aerosols emitted annually in China come from the Gobi desert and the adjacent plain plateau. Some studies discussed the size distribution of the dust aerosol in northern China (Ning *et al.*, 1995; Zhang *et al.*, 2003). These two studies demonstrated that the contribution of coarse aerosols to the high concentration of PM₁₀ significantly increased in the dusty seasons (i.e., winter and spring). The geometric mean diameter of the mass concentration spectra is reported to be 4.5 μm under dust storm conditions in desert areas, and the contribution of coarse aerosol to the mass concentration is approximately 65% at

Taiyuan (NC). In particular, the Loess Plateau (NWC, NC, ECn, and CSCn) is broadly located over the northern part of the Yangtze River and the desert area over north China, where long dry spells result in the frequent occurrence of dust every year (e.g., NWC: 50–100 days, NC: 10–30 days, ECn: approximately 10 days, and CSCn: up to 15 days).

In contrast, the southern part of the Yangtze River situated in East China (ECs) and Central South China (CSCs) are relatively humid areas with annual rainfall of 1200–1800 mm (<http://www.fas.usda.gov>). The other sub-regions [i.e., The northeast China (NEC) and Southwest China (SWC)] have a moderate annual precipitation of less than 1200 mm and a few dusty days (less than 5 days) every year. The aforementioned geographical and climatological characteristics of the 8 regions are summarized in Table 1.

3. Comparison of PM₁₀ concentration and MODIS aerosol optical thickness

By taking the average of the PM₁₀ and MODIS aerosol products for the analysis period, we obtained the spatial distributions of the annual-mean PM₁₀ concentrations, AOD_{0.55} (simply AOD hereafter), α , and η (Fig. 2). On the whole, the spatial patterns of the PM₁₀ concentration and MODIS AOD are comparable (Figs. 2a and 2b). A few observation sites in the CSCn, and SWC regions exhibit high PM₁₀ concentrations as well as high AOD values (c.f., PM₁₀ $\geq 130 \mu\text{g m}^{-3}$ and AOD ≥ 0.9), whereas the coastal areas of both the CSCs and ECs regions exhibit low PM₁₀ concentrations corresponding to low AOD (c.f., PM₁₀ $\leq 130 \mu\text{g m}^{-3}$ and AOD ≤ 0.7). However, dissimilar patterns appear particularly over the middle area of the NWC and NC regions, that is, very high PM₁₀ concentrations of more than $170 \mu\text{g m}^{-3}$ are observed along with low AOD values of less than 0.7. Further, moderate or high AOD values correspond to moderate or low PM₁₀ concentrations (c.f., AOD ≥ 0.7 and $90 \leq \text{PM} \leq 170 \mu\text{g m}^{-3}$) over the ECn region.

In order to examine if the spatial patterns of the PM₁₀ concentrations and MODIS AOD are related to the spatial locality with respect to the aerosol size distribution in China, we present the annual-mean

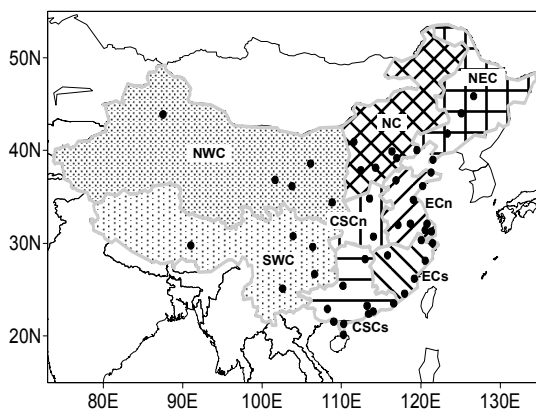


Fig. 1. Analysis domain and the location of 47 air quality monitoring sites.

Table 1. Geographical information and climatological characteristics in terms of the amount of annual precipitation and the frequency of dust event day of 8 sub-regions and 47 air quality monitoring sites in the main land of China.

Sub-Region	Occupied Province	Arid Area / Annual Precipitation (mm) **	Annual Dust days	The number of API Sites
North China (NC)	Beijing, Tianjin, Hebei, Shanxi, Inner Mongolia	Gobi Desert, Loess Plateau / 400–600	5–30	6
Northeast China (NEC)	Liaoning, Jilin, Heilongjiang	– / 600–800	< 5	4
East China				
Northern Yangzi River (ECn)	Shandong, Jiangsu, Anhui	Loess Area / 800–1200	< 10	10
Southern Yangzi River (ECs)	Zhejiang, Fujian, Jiangxi, Shanghai	– / 1200–1800	< 5	5
Central South China				
Northern Yangzi River (CSCn)	Henan, Hubei, Hunan	Loess Area / 800–1200	5–15	2
Southern Yangzi River (CSCs)	Guangdong, Guangxi, Hainan	– / 1200–1800	< 5	10
Southwest China (SWC)	Sichuan, Guizhou, Yunnan, Tibet	Tibet Plateau / <1200	–	5
Northwest China (NWC)	Shaansi, Guanu, Qinghai, Ningxia, Xinjiang	Taklimakan, Badain Jaran Desert, Loess Plateau / < 400	50–100	5

* Zhang *et al.* (1980) and Lie *et al.* (2004), ** <http://www.fas.usda.gov/>

MODIS \hat{a} and η (Figs. 2c and 2d). It is found that the low \hat{a} values are largely distributed over inland China, particularly the north and west China, which is consistent with η values. The places showing low values of \hat{a} and η , where coarse aerosol is dominant, are arid regions (NWC and NC) and agricultural regions (CSCn), while high \hat{a} and η values (both values ≥ 0.8 ; fine aerosol is dominant) are observed in the humid and mostly industrialized regions in the southern part of China (ECs and CSCs). Note that ECn (considered as an agricultural region) shows moderate \hat{a} and η values. Further, the η distribution indicates that the contribution of fine aerosol to AOD over land is apparently higher than that over the adjacent oceans: $\eta \geq 0.9$ in the east of China and South Korea, whereas $\eta \leq 0.7$ in the East Sea and East China Sea.

The most important inference from Fig. 2 is that the non-arid regions (i.e., ECs and CSCs), where fine aerosols dominate, reveal considerably analogous features between the observed PM10 concentration and MODIS AOD. In contrast, this similarity is not found in the arid regions (i.e., NWC and NC) where coarse aerosols dominate. It is also interesting to note that agricultural regions and most populated regions (i.e., ECn and CSCn) show significantly high AOD

values but a varying range of PM10 concentrations. For making these characteristics much clearer and considering the potential to establish a link between the PM10 concentrations and MODIS optical observations, we examine their temporal variations and present the results in the form of the spatial distribution of the correlation coefficient (Fig. 3) and the monthly time series (Fig. 4) for each sub-region.

To compare the seasonal variation between the PM10 concentrations and MODIS AOD, we depict the correlation coefficients of the time series of the two variables (Fig. 3). The moving average with a 60-day window was performed prior to the statistical calculation to avoid inter-seasonal noise. The statistical significance of the correlation is estimated using a two-tailed t-test with the degrees of freedom of $N/2L-2$, where N is the total number of data and $2L$ is the interval of e -folding autocorrelation (the degrees of freedom is of 10–20 ranges in the present data). Stations significant at the 90% level are indicated by filled symbols in Fig. 3. As seen in the figure, the spatial correlation pattern shows a distinct separation between the inland and southeast coastal region: a negative correlation in the inland region and a positive correlation along the southeast coast. Correlation coefficients of less than -0.6 are shown over dusty areas

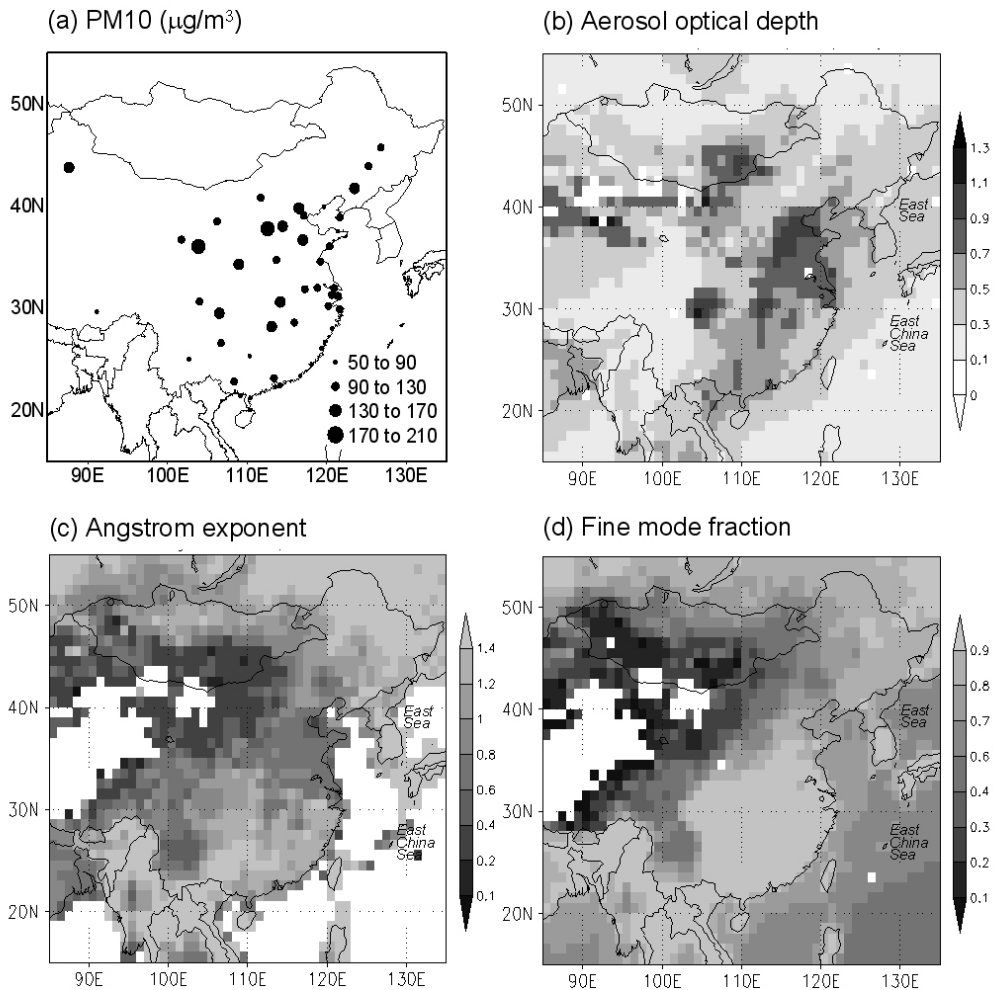


Fig. 2. Horizontal distribution of PM10 mass concentrations measured from each of the 47 sites (a), MODIS AOD (b), MODIS Å (c), and MODIS η (d). All values are obtained by averaging for the period 2003–2005.

(i.e., NWC and NC). Further, the moderately negative correlations (-0.3 to -0.6) exist in the agricultural and populated areas (i.e., CSCn and ECn). As mentioned earlier, the regions of NWC, NC, ECn, and CSCn located north of the Yangtze River show a precipitation of less than 1200 mm and between 10 and 100 dusty days every year. On the other hand, the sites with a positive correlation of more than $+0.3$ are located along the southeast coastal area (i.e., ECs and CSCs), where fine aerosols are dominant. These results of the simple correlation analysis for the temporal variation imply that the significant locality and the discrepancy between the values may be attributed to

the different size distributions and the different types of aerosols, which are associated with the characteristics of the land-cover, magnitude of human activity, and regional climate of each sub-region.

It should be noted that the factors mentioned above have a seasonal cycle. In particular, for example, over the ECn and CSCn regions with the highest population density in China, human activity is much more vigorous as compared to the surrounding regions. Therefore, the abundant anthropogenic emission of air pollutants can be accompanied with the better chance to have much more the secondary aerosols during the summer season. The secondary aerosols

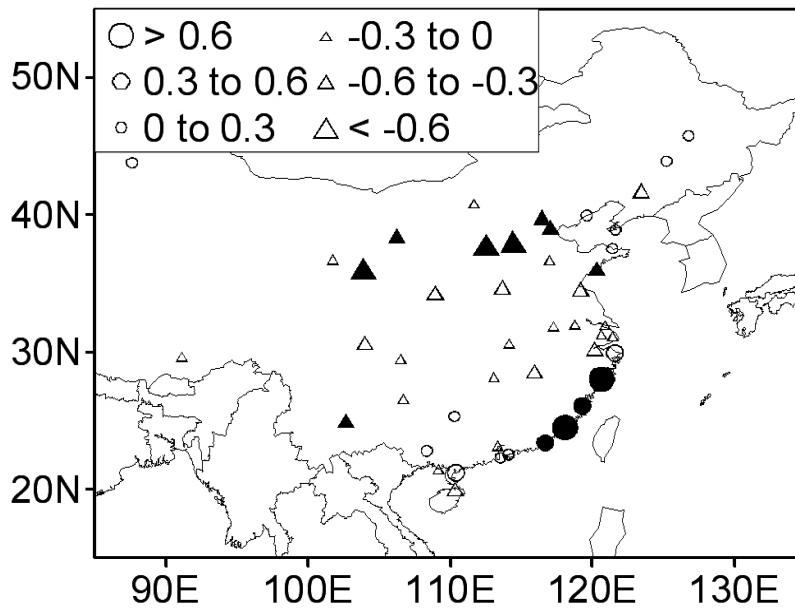


Fig. 3. Correlation coefficient between the MODIS AOD values and PM₁₀ mass concentrations at the 47 observational sites, where the circles and triangles of different sizes represent the positive and negative correlations of different magnitudes, respectively. Stations significant at the 90% level are filled.

are generally hygroscopic and their size can grow with high humidity in the summer, resulting in high mass extinction efficiency (Chin *et al.*, 2002). Moreover, these regions are widely occupied by cultivation areas that are barren in the winter season and easily emit relatively coarse dust particles during this period. Therefore, we focus on the seasonal variation at each sub-region.

Figure 4 shows the monthly variation in the PM₁₀ concentration, MODIS AOD, and η in some key regions, e.g., NWC (most arid region), NC (arid and partially populated region), ECn (agricultural and most populated region), and CSCs (non-arid region). First of all, it is evident that the observed PM₁₀ concentration show a strong maxima during winter in the NWC, NC, and ECn regions. The maximum values of the PM₁₀ concentrations in winter exceed $200 \mu\text{g m}^{-3}$ in the northern part (NWC and NC) and $120\text{--}140 \mu\text{g m}^{-3}$ in the eastern part (ECn). Observations of aerosols over Urumqi (87°E , 43°N , i.e., in NWC) also showed PM₁₀ concentrations in the order of winter>spring>fall>summer, and it was due to the heavy heating with coal combustion in winter (Li *et al.*,

2007). Also, more frequent occurrences of the stagnant weather conditions can result in the accumulation of atmospheric particles and high concentration episodes (He *et al.*, 2001; Chan and Yao, 2008). These high values of PM₁₀ concentrations in winter might be the primary cause of the strong negative correlation with the MODIS AOD values (Fig. 3). With regard to the observational results in this study, it can be explained that the coarse particles emitted from the very arid regions play an important role in enhancing the PM₁₀ concentrations in winter and spring in northern China, particularly NWC and NC. The η values in these two sub-regions exhibit very a small ratio — a range of 0.4–0.6. This supports the authors' explanation.

Second, the MODIS AOD values in the eastern China and the northern part of the Yangtze River shows strong maximum values in spring or summer, concurring with certain former studies (Chin *et al.*, 2002; Sun *et al.*, 2003). As seen in the figure, AOD values greater than 0.8 are found in the sub-regions of NC, ECn, and CSCs in that season. In general, highly populated areas coincide with the most culti-

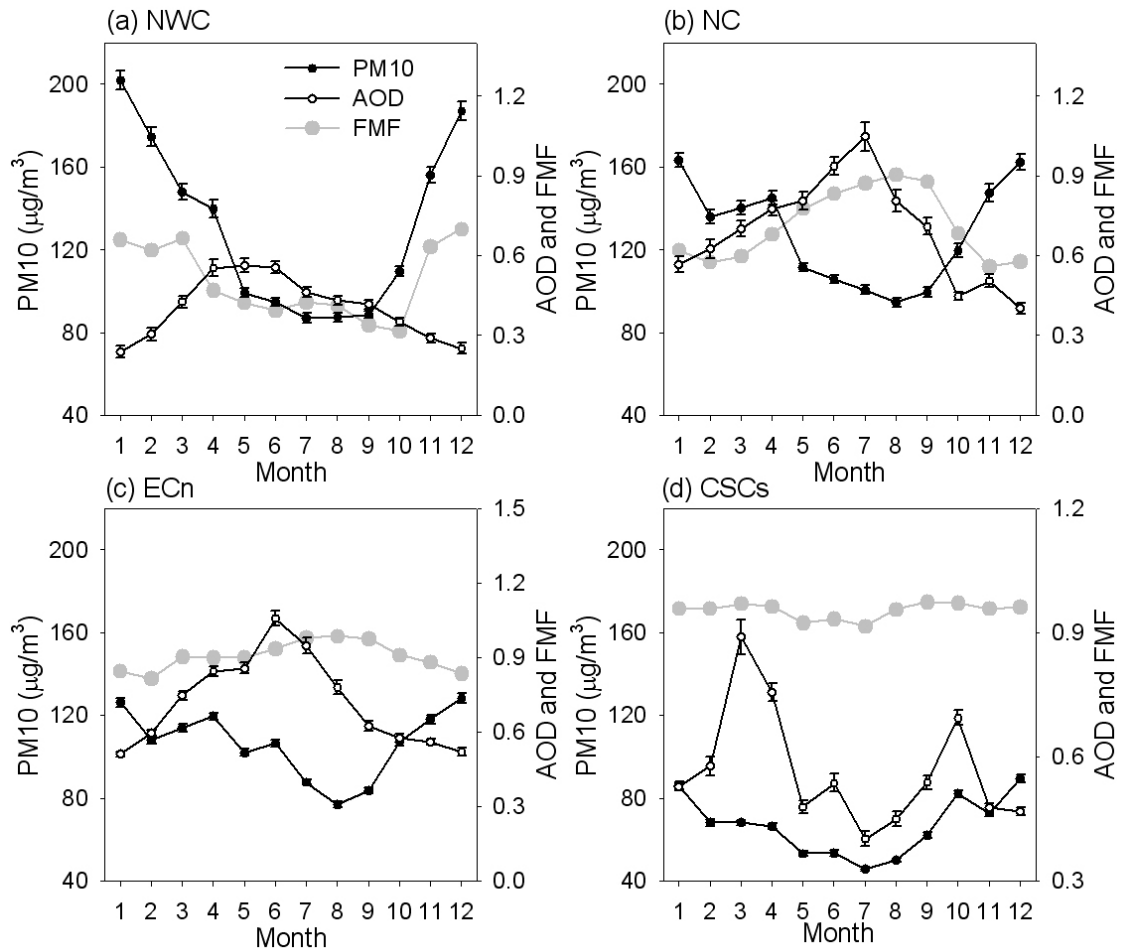


Fig. 4. Seasonal variation in the MODIS AOD, η , and PM₁₀ mass concentrations in four selected sub-regions: NWC, NC, ECn, and CSCs. The error bars correspond to the ± 1 standard errors of the AOD and PM₁₀ means.

vated, industrialized, vegetable covered regions in China. This indicates that high population density and developed economic condition are highly correlated with high AOD values, particularly in spring and summer. Subsequently, it seems that the ambient gas-phase air pollutants, which are abundantly emitted from these places, undergo excessive photochemical processes in the summer season for easy conversion into secondary aerosols. Moreover, high relative humidity would lead to high mass extinction efficiency of hygroscopic aerosols, so that the AOD values rise in summer as discussed below.

4. Discussion

We find that there is the evidential discrepancy between the MODIS AOD values and the PM₁₀ mass concentrations in China as well as the significant locality, as deduced from the spatial (Fig. 2) and temporal analyses (Figs. 3 and 4). Here, we discuss important scientific issues originating from the comparison between the PM₁₀ mass concentrations and MODIS optical products observed over China. The optical depth of PM₁₀ mass is indicative of solar light opacity. Light scattering is dependent on the size, type, and vertical profile of aerosol particles, all of which are influenced by both human activity and sea-

sonal variability of the regional climate.

More analytically, the relationship between the surface PM10 concentration and the total-columnar AOD is influenced by the following factors: the mass extinction efficiency (Chin *et al.*, 2002), relative contributions of different aerosol types to the total AOD, and the fractional AOD of the surface layer in the total-column value (van Donkelaar *et al.*, 2006). These factors vary spatiotemporally depending on the aerosol chemical composition, aerosol source, and atmospheric conditions in the boundary layer. Relative humidity increases the particle size of fine-mode hydrophilic aerosols and the mass extinction efficiency, readily making AOD more sensitive to the mass increase (Chin *et al.* 2002). Mineral dust dominates in the NWC arid region, while sulfate and carbonaceous aerosols dominate in the other regions. It is noted that mineral dust is very heavy but with low mass extinction efficiency, so that the PM10-AOD relation can be bothered with a few fine-mode aerosols (PM2.5) in the NWC arid region. The MODIS AOD values are therefore more sensitive to fine-mode aerosols than coarse-mode aerosols (Chu *et al.*, 2003; Wang and Christopher, 2003). The fractional AOD of the surface layer in the total-column value is generally invariable in China; However, it rises in the NWC arid region in spring due to wind-blown soil dust (Li *et al.*, 2008) and rises in the anthropogenic aerosol source regions (e.g., ECn, CSCn, and NC) in winter due to the accumulation of aerosols under the stagnant weather (He *et al.*, 2001; Chan and Yao, 2008). The high fractional AOD of the surface layer makes the more intimate the PM10-AOD relation.

In the regions (i.e., ECn, CSCn, and NC) intensively influenced by human activity, carbonaceous and secondary species (sulfate, nitrate, and ammonium) are the major contributors to the PM2.5 mass in the regions (Ye *et al.*, 2003; Chan and Yao, 2008). The AOD values are approximately greater than 0.6 with the η value being greater than 0.8 due to dominant anthropogenic fine-mode aerosols. The ratio of PM2.5 concentration to PM10 concentration is higher than other regions (around 60%), indicating significant contribution of anthropogenic aerosols to PM10 (Yu *et al.*, 2006). The seasonal difference of

PM2.5/PM10 ratio is consistent with the η value, i.e., lower in winter (~56%) than in summer (~60%) (Yu *et al.*, 2006). In the regions, high ratios (e.g., larger than 60%) are generally attributed to secondary particulate formation of species such as nitrate, sulfate, ammonium, and organics, while low ratios are attributed to the overwhelming contribution of fugitive dust or sand dust from long-distance transport (Xie *et al.*, 2005; Duan *et al.*, 2006; Sun *et al.*, 2006; Chan and Yao, 2008). The secondary aerosols transformed by the anthropogenic emission can exert a significant influence on the PM2.5 mass concentration rather on the PM2.5–10 concentration ($2.5 \mu\text{m} \leq d \leq 10 \mu\text{m}$). As noted, the increase in relative humidity from about 40% (the winter average) to 85% (the summer average) can increase the mass extinction efficiency for most hygroscopic aerosols by more than twice (Chin *et al.*, 2002). Therefore, the higher mass extinction efficiency and the higher mass concentrations of fine-mode aerosols in summer can cause higher AOD (see Figs. 4b and 4c). This is why PM10 mass concentration in the summer does not increase with the enhancement of the MODIS AOD values during the same period even in the highly populated and industrial areas of China.

Over the sub-regions of CSCs (Fig. 4d), the AOD values have maximum values in spring rather than summer, which would be associated with frequent rainfall due to the summer monsoon and the wind pattern mainly from the southeastern ocean where the air is clean. Furthermore, the relatively dry weather and a dominant wind from the north also contribute to the maximum value in spring. A similar pattern is found in the ECs region (not shown in Fig. 4). The major chemical compositions in CSCs are also carbonaceous aerosols and secondary species (about 65% of the total PM10 mass) (Chan and Yao, 2008). The average PM2.5 and PM10 concentrations were found to be high in winter than in summer in Pearl River Delta Region (Cao *et al.*, 2004), supporting almost fixed η values all the year round in Fig. 4d.

It should be also issued the determination of surface reflectance and the selection of the aerosol model adopted in MODIS. In inland China except for the ECs and CSCs coastal regions, MODIS AOD does

not match with very high PM₁₀ concentrations in the winter season. In addition to the discussion on the reasons for the occurrence of high PM₁₀ concentrations using the analysis of temporal variation (Figs. 3 and 4), the issue of a well-known limitation of the MODIS retrieval process in land area (Chu *et al.*, 2003; Hsu *et al.*, 2003; Kaufman *et al.*, 1997, 2002b; Remer *et al.*, 2005) should be considered as one of the reasons for the deficiency of MODIS AOD, particularly in arid regions, should be issued, i.e., the surface reflectance and aerosol model used. In order to account for the surface contribution, the MODIS aerosol retrieval process utilizes the reflectance measured at 2.1 μm , at which the fine-mode particles are transparent. In case of over the dust source area, the reflectance of 2.1 μm is usually more than the value of 1.5 in reflectance unit which is a critical value to determine whether to perform the retrieval process or not in operational sense (Chu *et al.*, 2003; Kaufman *et al.*, 1997, 2002b). It also was reported that the sparseness in the surface vegetation, existence of snow in winter, and dusty aerosols of large sizes could destroy the application of the so called “dark-target approach” as the first step to obtain the value of AOD in arid areas of the land. In order to figure out this problem, Hsu *et al.* (2004) suggested that the information obtained from the deep blue channel (0.41 μm) can provide a useful insight into dust plumes even over the bright surface after regulating the so called “trade-off” effect caused by absorption.

In comparison with the fine particles, the coarse dust aerosols in the source and its vicinity decrease the radiance at the top of atmosphere received by the satellite because of the significantly weaker light scattering. Therefore, the signal change caused by the aerosols becomes much smaller as compared to high surface reflectance values in the desert areas leading to large errors in the AOD values. According to the study of Bergin *et al.* (2001) performed for understanding the aerosol properties in Beijing during June 1999, the submicron aerosol attributed to 80% of the light scattering at 0.53 μm , while much larger particles ($>1.0 \mu\text{m}$) contributed to 80% of the mass concentration. The dependence of mass extinction on the size of aerosols can be ascertained using Fig.

3 of Chin *et al.* (2002), in which there is a significant drop in the mass extinction efficiency when the aerosol size is much greater than 2.5 μm . Those results indicate again that the MODIS AOD values obtained from a visible channel is more sensitive to the mass concentration of PM_{2.5} (including the transportable dust aerosol) rather than that of PM₁₀.

5. Concluding remarks

In China, the comparison between the PM₁₀ mass concentrations measured at 47 air quality monitoring sites and the MODIS aerosol properties was investigated for values measured over the last 3 years (2003–2005). It is revealed that the PM₁₀ mass concentration has a high correlation with MODIS AOD in the most developed and populated areas where fine-mode aerosols are dominant, while a strong negative correlation is observed over the most arid areas, which is the source of coarse dust aerosols. We also describe several factors that possibly explain the reason for the occurrence of these discrepancies. In north and northwestern China and the northern part of the Yangtze River, the large size of the particles enhances the PM₁₀ mass concentrations in the winter season; however, MODIS AOD cannot detect the maxima in winter because of the limitation of the aerosol retrieval process of MODIS for bright surfaces on land and the dependence of light scattering on the particle size and type. The secondary particle formation and the hygroscopic effect of anthropogenic species from human activities in the populated and industrialized areas of China may play an important role in the drastic increase in the MODIS AOD values in the spring and summer seasons, further, the summer monsoon affects the timing of the occurrence of the maxima of AOD in the Southeast China.

This study will be able to discuss several scientific issues in the study of aerosols and will be useful reference to improve the retrieval algorithm of the aerosol optical properties of satellites in China as well as to encourage other researchers to make use of the API in China as the nation-wide data sets in further research.

Acknowledgements. This study was funded by National Institute of Environmental Research, Korea. The MODIS data were obtained from GSFC DAAC.

REFERENCES

- Al-Saardi, J., J. Szykman, R. B. Pierce, C. Kittaka, D. Neil, D. A. Chu, L. Remer, L. Gumley, E. Prins, L. Weinstock, C. MacDonald, R. Wayland, F. Dimmick, and J. Fishman, 2005: Improving national air quality forecasts with satellite aerosol observations. *Bull. Amer. Meteor. Soc.*, **86**, 1249–1261.
- Bergin, M. H., G. R. Cass, J. Xu, C. Fang, L. M. Zeng, T. Yu, L. G. Salmon, C. S. Kiang, X. Y. Tang, Y. H. Zhang, and W. L. Charmeides, 2001: Aerosol radiative, physical and chemical properties in Beijing during June 1999. *J. Geophys. Res.*, **106**, 17969–17980.
- Cao, J. J., S. C. Lee, K. F. Ho, S. C. Zou, K. Fung, Y. Li, J. G. Watson, and J. C. Chow, 2004: Spatial and seasonal variations of atmospheric organic carbon and elemental carbon in Pearl River Delta Region, China. *Atmos. Environ.*, **38**, 4447–4456.
- Chan, C. K., and X. Yao, 2008: Air pollution in mega cities in China. *Atmos. Environ.*, **42**, 1–42.
- Chin, M., P. P. Ginoux, S. Kinne, O. Torres, B. N. Holben, B. N. Duncan, R. V. Martin, J. A., Logan, A. Higurashi, and T. Nakajima, 2002: Tropospheric aerosol optical thickness from the GOCART model and comparisons with satellite and sun photometer measurements. *J. Atmos. Sci.*, **59**, 461–483.
- Choi, Y.-S., C.-H. Ho, D. Chen, Y.-H. Noh, and C.-K. Song, 2008a: Spectral analysis of weekly variation in PM10 mass concentration and meteorological conditions over China. *Atmos. Environ.*, **42**, 655–666.
- _____, _____, J. Kim, D.-Y. Gong, and R. J. Park, 2008b: The impact of aerosols on the summer rainfall frequency in China. *J. Appl. Meteor. Climatol.*, **47**, 1802–1813.
- Chu, D. A., Y. J. Kaufman, G. Zibordi, J. D. Chern, J. Mao, C. Li, and B. N. Holben, 2003: Global monitoring of air pollution over land from the Earth Observing System-Terra Moderate Resolution Imaging Spectroradiometer (MODIS). *J. Geophys. Res.*, **108** (D21), 4661, doi: 10.1029/2002JD003179.
- Duan, F. K., K. He, Y. L. Ma, F. M. Yang, X. C. Yu, S. H. Cadle, T. Chan, and P. A. Mulawa, 2006: Concentration and chemical characteristics of PM2.5 in Beijing, China: 2001–2002. *Sci. Total Environ.*, **355**, 264–275.
- Engel-Cox, J. A., R. M. Hoff, A. and D. J. Haymet, 2004: Recommendations on the use of satellite remote-sensing data for urban air quality. *J. Air Waste Manage. Assoc.*, **54**, 1360–1371.
- _____, G. S. Young, and R. M. Hoff, 2005: Application of satellite remote sensing data for source analysis of fine particulate matter transport events. *J. Air Waste Manage. Assoc.*, **55**, 1389–1397.
- Gong, D.-Y., D. Guo, and C.-H. Ho, 2006: Weekend effect in diurnal temperature range in China: Opposite signals between winter and summer. *J. Geophys. Res.*, **111**, D18113, doi:10.1029/2006JD007068.
- _____, C.-H. Ho, D. Chen, Y. Qian, Y.-S. Choi, and J. Kim, 2007: Weekly cycle of aerosol-meteorology interaction over China. *J. Geophys. Res.*, **112**, D22202, doi: 10.1029/2007JD008888.
- He, K., F. Yang, Y. Ma, Q. Zhang, X. H. Yao, ...T. Chan, and P. A. Mulawa, 2001: The characteristics of PM2.5 in Beijing, China. *Atmos. Environ.*, **35**, 4959–4970.
- Hsu, N. C., S.-C. Tsay, M. D. King, and J. R. Herman, 2004: Aerosol properties over bright-reflecting source regions. *IEEE Trans. Geosci. Remote Sens.*, **42**, 557–569.
- Kaufman, Y. J., D. Tanré, L. A. Remer, E. Vermote, A. Chu, and B. N. Holben, 1997: Operational remote sensing of tropospheric aerosol over land from EOS Moderate Resolution Imaging Spectroradiometer. *J. Geophys. Res.*, **102**, 17051–17067.
- _____, _____, and O. Boucher, 2002a: A satellite view of aerosols in the climate system. *Nature*, **419**, 215–223.
- _____, N. Gobron, B. Pinty, J. Widlowski, and M. M. Verstraete, 2002b: Relationship between surface reflectance in the visible and mid-IR used in MODIS aerosol algorithm-Theory. *Geophys. Res. Lett.*, **29**, 2116, doi:10.1029/2001GL014492.
- Li, J., G. Zhuang, K. Huang, Y. Lin, C. Xu, and S. Yu (2007), Characteristics and sources of air-borne particulate in Urumqi, China, the upstream area of Asia dust. *Atmos. Environ.*, **42**, 776–787.
- Lie W., Q. Feng, T. Wang, Y. Zhang, and J. Shi, 2004: Physicochemistry and mineralogy of storm dust and dust sediment in Northern China. *Adv. Atmos. Sci.*, **21**, 775–783.
- Liu, Y., R. J. Park, D. J. Jacob, Q. Li, V. Kilaru, and J. A. Samat, 2004: Mapping annual mean ground-level PM_{2.5} concentrations using Multiangle Imaging Spectroradiometer aerosol optical thickness over the contiguous United States. *J. Geophys. Res.*, **109**, D22206, doi:10.1029/2004JD005025.
- Menon, S, J. Hansen, L. Nazarenko, and Y. Luo, 2002: Climate effects of black carbon aerosols in China and India. *Science*, **27**, 2250–2253.
- Ning, D. T., L. X. Zhong, and Y. S. Chung, 1996: Aerosol size distribution and elemental composition in urban

- areas of Northern China. *Atmos. Environ.*, **30**, 2335–2362.
- Remer, L. A., and coauthors, 2005: The MODIS aerosol algorithm, products, and validation. *J. Atmos. Sci.*, **62**(4), 947–973.
- Richter, A., J. P. Burrows, H. Nub, C. Granier, and U. Niemeier, 2005: Increase in tropospheric nitrogen dioxide over China observed from space. *Nature*, **437**, 129–132.
- Sun, D., Chen, J. Bloemendal, and R. Su, 2003: Seasonal variability of modern dust over the Loess Plateau of China. *J. Geophys. Res.*, **108**, 4665, doi:10.1029/2003JD003382.
- Sun, Y., G. Zhuang, A. Tang, Y. Wang, and Z. An, 2006: Chemical characteristics of PM_{2.5} and PM₁₀ in haze-fog episodes in Beijing. *Environ. Sci. Technol.*, **40**, 3148–3155.
- van Donkelaar, A., R. V. Martin, and R. J. Park, 2006: Estimating ground-level PM_{2.5} using aerosol optical depth determined from satellite remote sensing. *J. Geophys. Res.*, **111**, D21201, doi:10.1029/2005JD006996.
- Wang, J., and S. A. Christopher, 2003: Intercomparison between satellite-derived aerosol optical thickness and PM 2.5 mass: Implications for air quality studies. *Geophys. Res. Lett.*, **30**, 2095, doi:10.1029/2003GL-018174.
- Wang, M. X., R. J. Zhang, and Y. F. Pu, 2001: Recent researches on aerosol in China. *Adv. Atmos. Sci.*, **18**, 576–586.
- Xuan, J., and I. N. Sokolik, 2001: Characterization of sources and emission rates of mineral dust in Northern China. *Atmos. Environ.*, **36**, 4863–4876.
- Xie, S., T. Yu, Y. Zhang, L. Zeng, L. Qia, and X. Tang, 2005: Characteristics of PM₁₀, SO₂, NO_x and O₃ in ambient air during the dust storm period in Beijing. *Sci. Total Environ.*, **345**, 153–164.
- Ye, B., X. Ji, H. Yang, X. H. Yao, C. K. Chan, S. H. Cadle, T. Chan, and P. A. Mulawa, 2003: Concentration and chemical composition of PM_{2.5} in Shanghai for 1-year period. *Atmos. Environ.*, **37**, 499–510.
- Yu, J., T. Chen, B. Guinot, H. Cachier, T. Yu, W. Liu, and X. Wang, 2006: Characteristics of carbonaceous particles in Beijing during winter and summer 2003. *Adv. Atmos. Sci.*, **23**, 468–473.
- Zhang, X. Y., S. L. Gong, Z. X. Shen, F. M. Mei, X. X. Xi, L. C. Liu, Z. J. Zhou, D. Wang, Y. Q. Wang, and Y. Cheng, 2003: Characterization of soil dust aerosol in China and its transport and distribution during 2001 ACE-Asia: 1. Network observations. *J. Geophys. Res.*, **108**, 4261, doi:10.1029/2002JD002632.